View metadata, citation and similar papers at core.ac.uk
brought to you by CORE
provided by Qucosa - Publikationsserver der Universität Leipzig

diffusion-fundamentals
The Open-Access Journal for the Basic Principles of Diffusion Theory, Experiment and Application
www.diffusion-fundamentals.org, ISSN 1862-4138; © 2005-2008

# Li Dynamics in Amorphous $LiNbO_3$ as Probed by Solid State NMR on Different Length Scales

*Martin Wilkening,* Muayad Masoud, Paul Heitjans*

Leibniz Universität Hannover, Institut für Physikalische Chemie und Elektrochemie, and Zentrum für Festkörperchemie und Neue Materialien, Callinstr. 3a, 30167 Hannover, Germany

E-Mail: wilkening@pci.uni-hannover.de

*Presented on the Bunsen Colloquium: Diffusion and Reactions in Advanced Materials*
*September 27th – 28th, 2007, Clausthal-Zellerfeld, Germany*
*Keywords:* lithium niobate, Li diffusion, solid state NMR, stimulated echoes, amorphous ceramics

**Abstract.** Long-range Li diffusion parameters of amorphous $LiNbO_3$ are probed by $^7$Li two-time spin-alignment echo NMR spectroscopy which is sensitive to slow Li dynamics. The jump rates which were extracted from the spin-alignment echo decay curves exhibit Arrhenius behaviour between 293 K and 413 K. The activation energy (0.41(1) eV) is in good agreement with that of the high-temperature flank of the $^7$Li NMR spin-lattice relaxation rate peak. The latter was predicted to be about 0.4 eV when taking into account the frequency dependence of the corresponding spin-lattice relaxation rates on the low-*T* flank (see Wilkening et al., Phys. Chem. Chem. Phys. 4 (2002) 3246). Previous measurements of the spin-lattice relaxation rate had to be restricted to temperatures below 450 K in order to avoid crystallization of the material. Thus, only the low-temperature flank of the diffusion induced spin-lattice relaxation rate peak had been accessible yielding information about short-range Li diffusion.

## 1 Introduction

Lithium niobate ($LiNbO_3$) is currently one of the most intensively studied ferroelectric materials. Due to its excellent electro-optic, acousto-optic as well as its non-linear optic properties it is used in many important applications, *e.g.*, as photorefractive material for optical waveguides in telecommunication. In many of these applications various diffusion processes are important. In general Li diffusion plays an important role in developing new electrode materials for secondary ion batteries. Recent investigations by impedance and $^7$Li NMR spectroscopy revealed that the room temperature Li conductivity in amorphous $LiNbO_3$ is by about a factor of $10^6$ higher than that in the corresponding poly- as well as single-crystalline material [1]. It is an ideal model system to show that the introduction of disorder can lead to a dramatic increase of ionic mobility.

The Li hopping process in amorphous $LiNbO_3$ was investigated previously by temperature and frequency dependent measurements of the $^7$Li NMR spin-lattice relaxation (SLR) rate

 © 2008, M. Wilkening

($1/T_1$) in the laboratory frame [2]. Due to the thermal sensitivity of amorphous $LiNbO_3$ to crystallization these investigations had to be restricted to temperatures below 450 K. Up to this temperature only the low-temperature flank of the diffusion induced relaxation rate peak could be partly observed. This means that only short-range diffusion parameters were accessible by $^7$Li NMR relaxation. The corresponding high-temperature flank, however, yields information about long-range parameters [3]. The frequency dependence of the low-$T$ rate $1/T_1$ was used to predict the long-range activation energy $E_A$ of SLR-NMR. According to this prediction $E_A$ should be around 0.4 eV, see ref. [2].

Analogous measurements in the rotating frame probing diffusion on a longer length scale would shift the position of the corresponding relaxation rate peak to lower temperatures. However, these measurements failed in the present case because of a drastic increase of the so-called non-diffusive background relaxation rate covering any diffusively induced contribution to the corresponding rate in the rotating frame, $1/T_{1\rho}$.

In the present paper $^7$Li stimulated echo NMR, see *e.g.*, refs. [4-7] for details of the method, is used to study Li dynamics in amorphous $LiNbO_3$. The method is capable of probing Li dynamics on a longer length scale at moderate temperatures [8,9], i. e., below 450 K in the present case. Results from $^7$Li stimulated echo NMR are compared with activation energies obtained by $^7$Li SLR-NMR spectroscopy (in the laboratory frame) and dc-conductivity measurements taken from the literature. As the methods probe Li dynamics on different length scales they do not necessarily give the same results. Especially in an amorphous solid with a non-homogenous behaviour concerning Li diffusion, time-scale dependent activation energies are expected.

## 2 Experimental

Amorphous $LiNbO_3$ was prepared following a sol-gel routine from $LiNb(OEt)_6$ dissolved in ethanol. The same sample was used previously for a spin-lattice relaxation NMR study, see ref. [2]. Cf. also ref. [2] for details of sample preparation. It cannot be excluded that the sample still contains a small amount of organic residuals. The sample is X-ray amorphous and consists of particles with diameters of 1 to 20 mm. A sample heated at 720 K shows the typical diffraction pattern of pure phase $LiNbO_3$ [10].

$^7$Li stimulated echoes (spin-alignment echoes, SAE) were measured using the three-pulse sequence introduced by Jeener and Broekaert [11]: 90° – $t_p$ – 45 ° – $t_m$ – 45°. The first two pulses, separated by the preparation time $t_p$ (10 µs … 100 ms), are used to generate spin-alignment order which decays during the subsequent period whose duration is determined by the mixing time $t_m$ (10 µs … 100 s). The last pulse converts spin-alignment order into an observable transverse magnetization. The spin-alignment echo is detected at $t = t_p$ directly after the 45° reading pulse. The echo amplitude $S_2$ is recorded at fixed $t_p$ and for variable $t_m$ as a function of temperature. We have used a Bruker MSL 100 and an MSL 400 solid state spectrometer for the measurements. The spectrometers are connected to a field-variable Oxford cryomagnet (MSL 100) for measurements at $\nu$ = 39 MHz and 78 MHz, and to a shimmed Oxford cryomagnet at fixed field (MSL 400) corresponding to a $^7$Li resonance frequency $\nu$ of 155 MHz, respectively. The 90° pulse length was about 5 µs in both cases. Up to 64 scans were accumulated for each spin-alignment echo. The recycle delay was at least 5 $T_1$. The spin-lattice relaxation rates $1/T_1$ were measured using the well-known saturation pulse sequence [12]. The sample was sealed in a quartz tube under vacuum. The temperature near the sample was controlled (± 2 K) via an Oxford ITC using a Ni-CrNi thermocouple.

 © 2008, M. Wilkening

## 3 Results and Discussion

The decay of spin-alignment echo NMR correlation functions $S_2$ is either caused by quadrupolar spin-lattice relaxation or due to slow Li jumps between electrically inequivalent Li sites. Inequivalence means that the sites involved in the hopping process are labelled by different quadrupole frequencies $\omega_q$. The quadrupole frequency $\omega_q$ results from the interaction of the quadrupole moment of the $^7$Li nucleus (spin-3/2 probe) with a non-vanishing electric field gradient produced by the electric charge distribution of the neighbouring ions at the Li site. The mobile $Li^+$ ions experience site-specific electrical interactions and thus, from the point of view of a jumping ion, $\omega_q$ becomes a function of $t_m$ leading therewith to a damping of the echo amplitude $S_2$. The temperature dependence of the decay constant ($1/\tau_{SAE}$) of the corresponding correlation function $S_2(t_m)$, which usually can be described by a stretched exponential, can be used directly to probe slow Li hopping processes. By using $^7$Li SAE-NMR the upper limit of accessible decay constants is given by the spin-spin relaxation rate which is typically of the order of $10^4$ $s^{-1}$. The lower limit is given by the (quadrupolar) spin-lattice relaxation rate which is usually of the order of a few seconds.

Using a short preparation time is a necessary pre-condition to ensure that mainly spin-alignment order is created after the first two rf-pulses of the Jeener-Broekaert pulse sequence [13]. Only in this case a (two-time) single particle correlation function $S_2$ is obtained. $^7$Li spin-alignment echoes at 373 K and fixed $t_m$ but for variable preparation times are shown in Fig. 1.

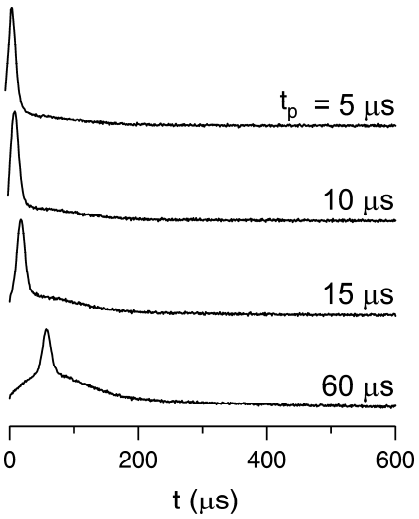


**Fig. 1:** $^7$Li NMR echoes recorded with the Jeener-Broekaert pulse sequence at fixed mixing time $t_m$ = 10 μs but for variable preparation times $t_p$ as indicated. The results were obtained at 373 K and 155 MHz.

Whereas at short $t_p$ mainly quadrupolar order is created (fast decaying part of the echo), at larger preparation time, see *e.g.* the echo at $t_p$ = 60 μs, dipolar contributions increasingly become important (slowly decaying part of the echo). If not stated otherwise, $t_p$ = 10 μs was used for all experiments. Fourier transformation (Fig. 2) of the stimulated echoes is helpful to clarify the impact of homonuclear dipole-dipole interactions on the echo formation at various preparation times. Although the spin-alignment spectrum recorded at $t_p$ = 10 μs is dominated by a broad Gaussian shaped quadrupole part, central components are visible even at very short $t_p$ = 10 μs. However the latter take only 13 % of the total area. In order to study the evolution of dipolar contributions, we have read out the spin-alignment echo intensity either at $t = t_p$ and at $t' = t_p + 70$ μs. Due to the fast decay of the spin-alignment echo intensity the signal intensity determined at $t'$ only reflects dipolar contributions. The result for $T$ = 389 K and 373 K is shown in Fig. 3. A similar behaviour was found previously for other Li conductors [14]. Whereas at short $t_p$ the spin-alignment echo intensity is already maximal, the weaker dipolar contribution reaches its maximum at around 100 μs at 373 K. At 400 μs the echo and its Fourier transform is exclusively composed of a sharp resonance resulting from homonuclear dipo-

 © 2008, M. Wilkening

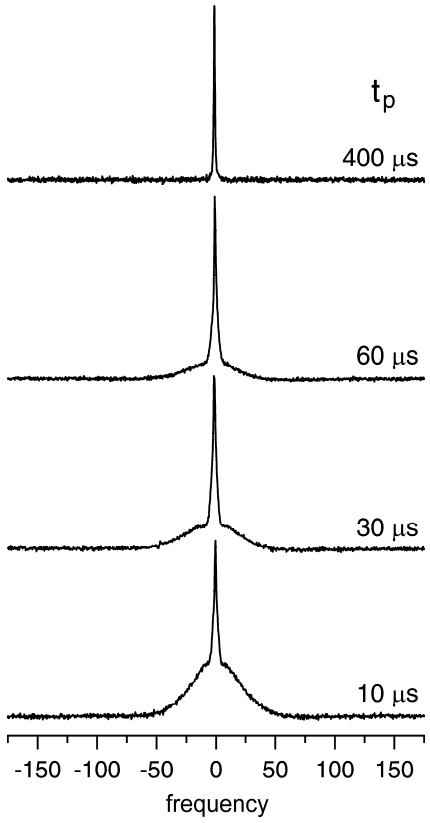


**Fig. 2:** $^7$Li stimulated echo spectra (373 K, 155 MHz) recorded at $t_m$ = 10 µs and variable $t_p$ as indicated. With increasing preparation time the broad quadrupole contribution disappears and the spectra are increasingly governed by homonuclear dipole-dipole interactions (sharp line).

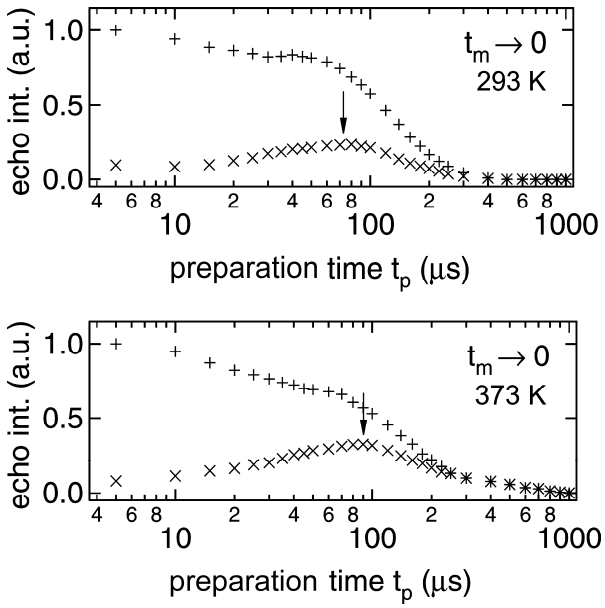


**Fig. 3:** Stimulated echo intensity as a function of $t_p$ read out at $t = t_p$ (+) and at $t' = t_p + 70$ µs (×), respectively for two temperatures. The latter one represents the dipolar contributions to the echo. Only at short $t_p$ a sufficiently good separation of both parts is possible.

lar interactions. The decay constant of the quadrupole part is roughly obtained when the data points at $t'$ are subtracted form those determined at $t = t_p$. The resulting decay curve $S_2(t_p) \propto \exp(-t_p / T_{2,\mathrm{SAE}})$ yields $T_{2,\mathrm{SAE}} \approx 55\,\mu$s.

$^7$Li SAE-NMR amplitudes, $S_2(t_p = 10\ \mu\mathrm{s}, t_m)$, vs. $t_m \cdot T$ recorded at 155.5 MHz and at various temperatures are shown in a semi-logarithmic plot in Fig. 4. The solid lines in Fig. 4 represent fits with stretched exponentials, $S_2(t_p = 10\ \mu\mathrm{s}, t_m) \propto \exp(-(t_m / \tau_{\mathrm{SAE}})^{\gamma})$. The stretching

 © 2008, M. Wilkening

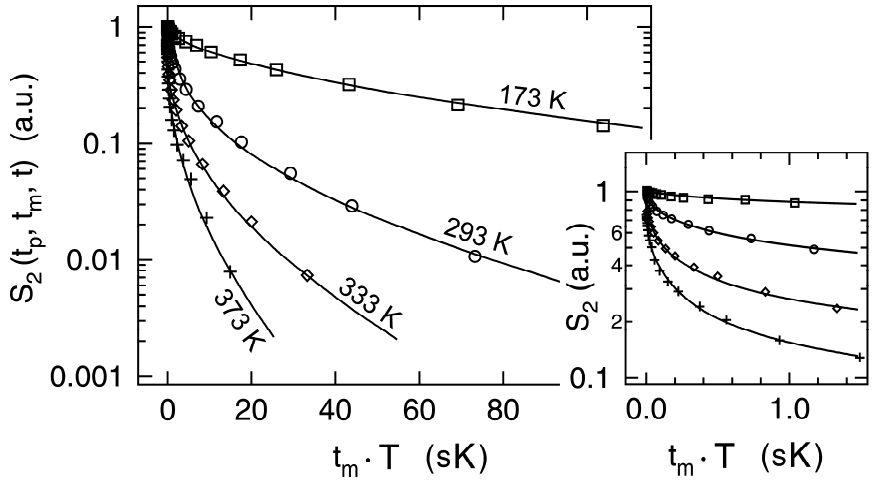


**Fig. 5:** Two-time correlation functions ($S_2(t_p = 10\ \mu s, t_m)$ vs. $t_m \cdot T$) of amorphous $LiNbO_3$ measured at 155 MHz and for various temperatures. The inset shows the shape of the correlation functions at smaller values $t_m \cdot T$.

exponent $\gamma$ ranges from 0.6 to 0.25 between $T$ = 150 K and 450 K. $\gamma$ is constant up to $T$ = 200 K and decreases then linearly with decreasing1/$T$. Strongly stretched hopping correlation functions might be due to the presence of a distribution of jump rates in amorphous $LiNbO_3$. The corresponding decay rates, partly measured at different resonance frequencies (39, 78 and 155 MHz), are shown in Fig. 5.

Below about 200 K ($\gamma$ = const., see above) the $S_2$ decay is dominated by spin-lattice relaxation effects because of two reasons: i) $1/\tau_{SAE}$, although much larger than $1/T_1$, shows the same weak temperature dependence as the corresponding SLR rates and ii) $1/\tau_{SAE}$ depends on frequency as is also found for $1/T_1$, which reflects the non-diffusive background rates in this temperature range [2]. Between 200 K and 300 K a crossover regime is found leading to the temperature range where $1/\tau_{SAE}$ finally follows Arrhenius behaviour with $E_A$ = 0.41(1) eV, cf. ref. [15]. In this $T$-range the $S_2$-decay is induced by slow Li jumps in amorphous $LiNbO_3$. Taking into account the background effects, *i. e.*, extrapolating the low-$T$ values of $1/\tau_{SAE}$ to higher $T$ and subtracting the extrapolated rates from the measured ones, the activation energy increases to 0.46(2) eV. As expected for a correlation rate, above 300 K the $S_2$ decay constant

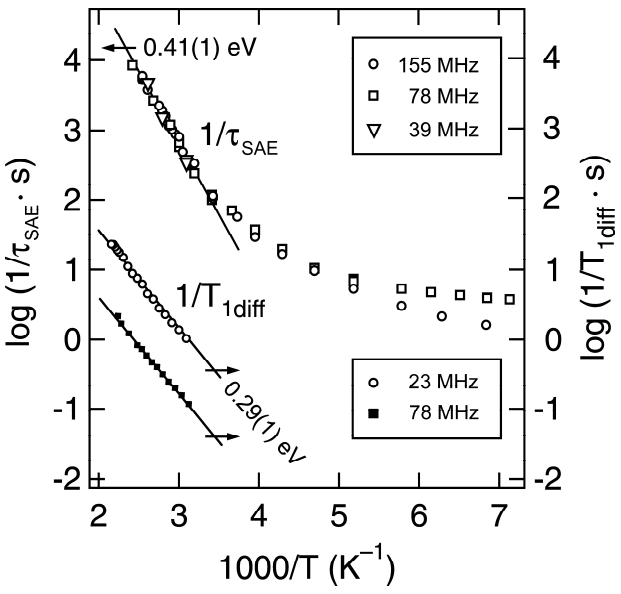


**Fig. 6:** $^7$Li SAE-NMR decay rates $1/\tau_{SAE}$ vs. $1/T$. Between room temperature and 400 K the data points were recorded at three different resonance frequencies as indicated. For comparison, diffusion induced SLR rates $1/T_{1\ diff}$ vs. $1/T$ (measured in the laboratory frame for $\nu$ = 23 MHz and 78 MHz) are shown, too. The solid lines represent linear fits and lead to the activation energies shown.

 © 2008, M. Wilkening

is independent of the resonance frequency ν. This is in contrast to $1/T_{1\,\mathrm{diff}}$ which generally depends on frequency (*cf.* ref. [2]). In the present case $1/T_{1\,\mathrm{diff}} = \nu^{-\alpha}$ with $\alpha = 1.7(2)$ was found [2]. Ideal Bloembergen-Purcell-Pound (BPP) behaviour [16], implying random isotropic diffusion, would lead to $\alpha = 2$. Values of $\alpha$ in the range $1 \leq \alpha < 2$ indicate that the hopping process is influenced by structural disorder and/or Coulomb interactions between the hopping ions which is assumed by several models [17-19]. Below 500 K only the low-temperature flank of the $1/T_{1\,\mathrm{diff}}(1/T)$ peak is accessible reflecting short-range Li motions. The activation energy of the low-temperature flank at 23 MHz is $E_A^{lT} = 0.29(1)$ eV (Fig. 6). The corresponding value of the high-$T$ flank, $E_A^{hT}$, which is sensitive to long-range Li diffusion, is linked with $E_A^{lT}$ via the expression $E_A^{lT} = (\alpha - 1)E_A^{hT}$, see *e.g.* [20]. Thus, from the low-$T$ frequency dependence of $1/T_{1\,\mathrm{diff}}$ an activation energy $E_A^{hT} = 0.41(7)$ eV is roughly predicted. This is in good agreement with the measured value using $^7$Li stimulated echo NMR between 300 K and 400 K. Activation energies of amorphous $LiNbO_3$ from dc-conductivity measurements range between 0.4 and 0.6 eV depending on the preparation route, see *e.g.*, Refs. [1,21,22]. Table 1 summarizes the results obtained from various methods probing Li diffusion on different length scales. It points out the heterogeneous nature of Li transport in a disordered material and corroborates our previous result that SAE-NMR provides a microscopic access to the long-range activation energy [9].

**Table 1:** Activation energies $E_A$ of the Li diffusivity in amorphous $LiNbO_3$ as probed by different methods

| Method | SLR-NMR | $^7$Li NMR line shapes | SAE-NMR | dc-conductivity |
|---|---|---|---|---|
| $E_A$ (eV) | 0.27 … 0.29(1); [2] | ≈ 0.35; [2] | 0.41(1); [15]<br>0.46(2); see text | 0.4 … 0.6; [1,21,22] |

## 4 Conclusion

The present comparison of experimental results about Li diffusion in a disordered model substance like amorphous $LiNbO_3$ shows that $^7$Li stimulated echo NMR technique is highly capable to complement frequency dependent relaxation NMR methods to study Li dynamics in solid ionic conductors. As it probes slow Li motions, SAE-NMR usually does not require high temperatures so that diffusion parameters on a longer length-scale are accessible via a microscopic NMR technique at moderate temperatures. The technique is applicable to a large number of Li conductors. In the present case, the SAE-NMR activation energy is in fair agreement with that which was roughly predicted by the frequency dependence of the diffusion induced spin-lattice relaxation rate of the low-$T$ flank. Interestingly, although the two methods probe different correlation functions, consistent results are obtained.

### References

[1] P. Heitjans, M. Masoud, A. Feldhoff, M. Wilkening, Faraday Discuss. 134 (2007) 67.
[2] M. Wilkening, D. Bork, S. Indris, P. Heitjans, Phys. Chem. Chem. Phys. 4 (2002) 3246.
[3] P. Heitjans, S. Indris, M. Wilkening, Diffusion Fundamentals 2 (2005) 45.
[4] M. Wilkening, W. Küchler, P. Heitjans, Phys. Rev. Lett. 97 (2006) 065901.
[5] M. Wilkening, P. Heitjans, J. Phys.: Condens. Matter 18 (2006) 9849
[6] F. Qi, G. Diezemann, H. Böhm, J. Lambert, R. Böhmer, J. Magn. Res. 169 (2004) 225.
[7] R. Böhmer, J. Magn. Res. 147 (2000) 78.
[8] M. Wilkening, R. Amade, W. Iwaniak, P. Heitjans, Phys. Chem. Chem. Phys. 9 (2007) 1239.
[9] M. Wilkening, C. Mühle, M. Jansen, P. Heitjans, J. Phys. Chem. B 111 (2007) 8691.
[10] M. Wilkening, Ph.D. thesis, Universität Hannover, 2005.
[11] J. Jeener, P. Broekaert, Phys. Rev. 157 (1967) 232.
[12] E. Fukushima, S. B. W. Roeder, Experimental Pulse NMR, Addison-Wesley, Reading, 1981.
[13] X.-P. Tang, Y. Wu, J. Magn. Res. 133 (1988) 155.

 © 2008, M. Wilkening

[14] F. Qi, T. Jörg, R. Böhmer, Solid State Nucl. Magn. Res. 22 (2002) 484.
[15] M. Wilkening, P. Heitjans, Solid State Ionics 177 (2006) 3031.
[16] N. Bloembergen, E. M. Purcell, R. V. Pound, Phys. Rev. 73 (1948) 679.
[17] K. L. Ngai, O. Kanert, Solid State Ionics 53 (1992) 963.
[18] K. Funke, Prog. Solid State Chem. 22 (1993) 11.
[19] A. Bunde, P. Maass, M. Meyer, in: P. Heitjans and J. Kärger (Eds.), Diffusion in Condensed Matter - Methods, Materials, Models, Springer, Berlin, 2005.
[20] P. Heitjans, A. Schirmer, S. Indris, in: P. Heitjans and J. Kärger (Eds.), Diffusion in Condensed Matter - Methods, Materials, Models, Springer, Berlin, 2005.
[21] A. Glass, K. Nassau, T. Negran, J. Appl. Phys. 49 (1978) 4808.
[22] S. Ono, H. Mochizuki, S. Hirano, J. Ceram. Soc. Japan 104 (1996) 574.

 © 2008, M. Wilkening